TRIBOLOGY METHODS

Space Tribometers: Design for Exposed Experiments on Orbit

Brandon A. Krick · W. Gregory Sawyer

Abstract Eight pin-on-disk tribometers have been made for testing materials in space on board the International Space Station. They will be exposed directly to the low earth orbit (LEO) environment on board the "Materials on the International Space Station Experiments" platform where they will experience extreme conditions including atomic oxygen, ultrahigh vacuum, radiation (including UV radiation), and thermal ranges from −40 to 60 °C. In order to survive launch and LEO, these tribometers were designed to be extremely compact, rugged, and reliable. Pin-on-disk tribology experiments are now being performed with a 13.2 mm/s sliding velocity (14 RPM at 9 mm wear track radius) and a 1 N normal load with hemispherical pin of 1.5875 mm radius. Materials tested include $MoS_2/Sb_2O_3/Au$, $MoS_2/Sb_2O_3/C$, $YSZ/Au/MoS_2/DLC$, and SiO-doped DLC coatings, and bulk samples of polytetrafluoroethylene (PTFE) alumina nanocomposites and gold.

Keywords Space tribology · Tribometers · Aerospace · Coating · Solid lubricants · Low earth orbit

1 Introduction

Existing and future moving mechanical assemblies for aerospace applications depend upon the maintenance free, low friction, and low wear operation of solid lubricants and coatings of contacting surfaces. The space environment is harsh, with a wide range of thermal extremes, ultrahigh vacuum, atomic oxygen, solar radiation (including destructive ultraviolet radiation), and micro meteoroids; this was recently reviewed in the January 2010 MRS Bulletin [1]. These environmental conditions collude to make most traditional lubrication strategies and intuitions gained from terrestrial tribology dubious. There remains a desire to better understand the effects of the space environment on materials and the tribological behavior of materials in that environment.

Historically, the observations of material degradation as observed on returning spacecraft motivated the studies of the space environment and its deleterious effects on most materials. Over the past half-decade many exposure and flight experiments have been devoted to understand this space environment and explore the possibility of terrestrial laboratory recreation of these conditions. One of the first extensive materials exposure experiments in space was NASA's Long Duration Exposure Facility (LDEF). Since then, there have been a number of exposure experiments including experiments from the European Space Agency (ESA), Japan Aerospace Exploration Agency (JAXA), and the National Aeronautics and Space Agency (NASA) (recently reviewed by Edwards [2]).

The needs for durable and high performance spacecraft are increasing, and tribological materials remain at the forefront of materials development efforts. Eight pin-on-disk tribometers were designed, constructed, and flown as part of the seventh Materials on the International Space Station Experiments (MISSE 7) platform. MISSE 7 is the seventh of a series of experiments designed to provide the community with a platform to perform experiments in the harsh low earth orbit (LEO) environment [3–5]. This ambitious seventh MISSE program includes several active experiments, which actively collect data on orbit and many passive experiments (exposure experiments that are

B. A. Krick · W. G. Sawyer (✉)
Department of Mechanical and Aerospace Engineering,
University of Florida, Gainesville, FL 32611, USA
e-mail: wgsawyer@ufl.edu

analyzed in the lab upon mission completion with no active data acquisition on orbit) including solar arrays, tribometers, optical samples, spectrometers, and others [6].

The development of tribometers for use in space has resulted in a compact and robust tribometer; this tribometer design is versatile and can be used by others in the tribology community to carry out experiments in vacuum and other challenging environments. Further, these tribometers are compact enough to be relatively easily coupled to various in situ surface analysis techniques [7, 8], including Scanning Electron Microscopes (SEM), X-ray Photoelectron Spectroscopy (XPS), Raman spectroscopy, and others. This manuscript will discuss the design constraints from LEO and the resulting design of the tribometer hardware.

2 Low Earth Orbit Environment

The common perception of space is ultrahigh vacuum and low gravity; however, LEO consists of a particularly aggressive environment. The International Space Station is in LEO $\sim$ 350 km above the earth's surface and is moving at $\sim$ 27,700 km per hour. At this altitude the environment contains a substantial pressure of atomic oxygen, solar UV radiation (Fig. 1a, b), ionizing radiation, thermal cycling (−40 to 60 °C), and micrometeoroids and debris [1]. The ultrahigh vacuum levels so commonly thought of as the space environment are only expected to be experienced on the 'wake' surface (trailing surface) of the experiments. Fig.1c summarizes the conditions of LEO as expected for the MISSE 7 mission.

Atomic oxygen is the most prevalent molecular species in LEO and is generated by the breakdown of molecular oxygen (O_2) by UV radiation. It has been proven to be highly destructive to surfaces, oxidizing and degrading metals, polymers, and other materials in the LEO environment [9]. Owing to the high orbital speed of the International Space Station, the atomic oxygen (impact energy $\sim 4.5 \pm 1$ eV) is impinging the 'ram' surface (leading surface) at a rate of 10^{14}–10^{15} atoms/(cm^{2}s) while the trailing surface is in the 'wake' and is effectively devoid of atomic oxygen exposure [10].

A much broader frequency and higher spectral intensity of light exists in the extraterrestrial environment, particularly on the UV side of the spectrum [11, 12]. This radiation can be damaging too many materials and in particular is known to degrade polymeric materials [13].

Temperatures of the experiments will continuously change as the experiments cycle into and out of direct exposure to the sun. Based on the positioning of these experiments on the International Space Station, the predicted temperature range of the experiments is from −40 to +60 °C as given by the MISSE 7 mission constraints.

Designing for thermal expansion over this range of temperatures and selecting electronics is a typical design challenge of space.

3 Tribometer Design

3.1 Constraints

Due to the limited size of the passive experiment carriers used on MISSE 7, the high cost of space missions, and the limited real estate allotted for tribometers, the design and packaging was constrained to two 60 mm×100 mm footprints with a height of 50 mm. In each 60 mm×100 mm space we designed and packaged four rotating pin-on-disk tribometers. One group of four was designated as the 'ram' experiments and another group of four was designated as the 'wake' experiments.

Launch vibrations are over eight g's during certain periods of the Space Shuttle's $\sim$ 8-min ride to orbit. Based on the MISSE 6 vibration conditions, the following random vibration accelerations will be seen by the tribometers: *translational accelerations* (N_x= ±8.8 g, N_y= ±10.6 g, and N_z= ±8.1 g), and *rotational accelerations* (R_x= ±195 rad/s^2, R_y= ±60 rad/s^2, and R_z= ±80.0 rad/s^2) relative to the coordinate system defined in Fig. 1c. The Miles equation, a single degree of freedom solution to random vibration that allows us to approximate the random vibrations with a very conservative 3σ design estimate of 60 g's, was used to simulate these random vibrations applied to our tribometers [14]. Instrumentation for force measurement typically relies on sensible flexibility; thus, these vibrations constrain designs to use light, stiff, and strong components.

The entire set of MISSE experiments was allocated 289 W nominal and 410 W maximum electrical power draw. In addition, the human element is not absent in space; the designs were also required to withstand a 'kick-load' of 560 N from the astronauts, and not puncture or cut the space-suits. Sharp corners and edges are not allowed and any edge must have fillets greater than 1 mm or be completely round (any exposed corners must have a radius of 13 mm).

3.2 Targeted Experimental Conditions

Although the tribometers are capable of operating over a wide range of normal loads and rotational speeds, nominal operational parameters were assigned for this mission. As this is the first opportunity for this type of experiment, parameters were assigned to be somewhat representative of the contact pressures and sliding velocities seen in many space applications and laboratories. The conditions were also picked such that they are repeatable in laboratory tribological testing. The nominal operating parameters are:

Fig. 1 The MISSE 7 tribometers will experience a variety of harsh conditions while in low earth orbit. They will be exposed to solar radiation, UV radiation (**a**) and (**b**), and atomic oxygen while facing the 'ram' direction of the International Space Station in contrast to being in ultrahigh vacuum while facing the 'wake' direction (**c**)
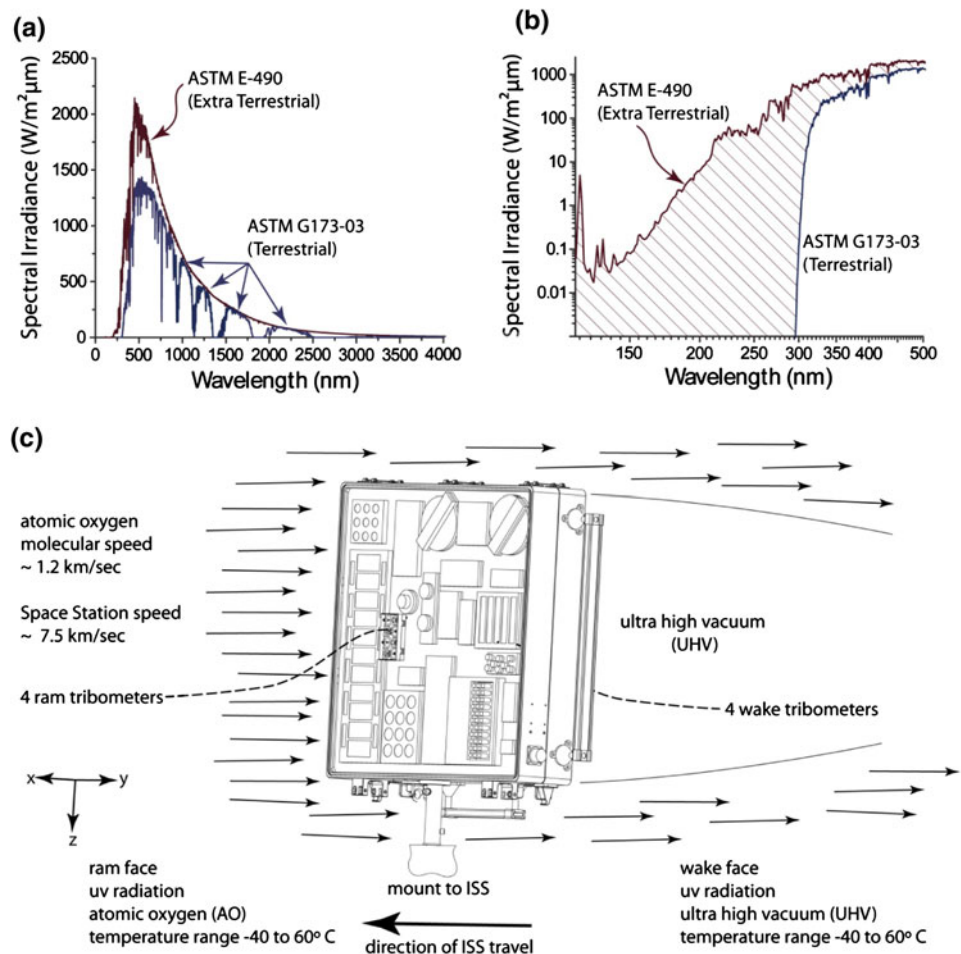
- Normal force ∼ 1 N (varies slightly from sample to sample)
- Pin radius of 1.6 mm
- Wear track radius 9 mm
- Rotational disk speed 14 RPM ± 0.05
- Linear sliding speed 13.2 ± 0.1 mm/s

3.3 Tribometer Assembly and Components

A pin-on-disk tribometer was selected because of the simplicity and ubiquitous nature of the design. The tribometer uses a piezo-electric actuator to pull a monolithic biaxial force transducer into contact with the spinning disk, and to prevent contact with the disk when it is not energized. The flexure pivots and loads a spherically capped pin onto the disk. The disk is rigidly mounted to a spindle with a 157:1 gear head driven by a vacuum compatible DC motor. The normal and tangential forces focus strains at flexure points on the monolithic flexure and are measured via strain gages. This is shown schematically in Fig. 2a.

3.3.1 Monolithic Biaxial Force Transducer and Loading Flexure (or Flexure)

The monolithic flexure acts as the normal and friction force transducer, as well as the pin holder. The two orthogonal cantilever beams are instrumented with four strain gages in a full Wheatstone bridge configuration. The flexure was made of Ti_6Al_4V due to its high strain to failure and strength to weight ratios. The instrumented cantilever beam portions of the flexure are 0.5 mm thick, 5 mm wide, and 8 mm long. A set screw holds a 3.175 mm hemispherical pin at the end of the flexure. The piezoelectric actuator is mounted near the pivot of the flexure to amplify the displacements and accommodate wear during testing.

3.3.2 Piezo-Electric Actuator Assembly

A custom piezo actuator was purchased from Cedrat technologies that can displace a maximum distance of 150 μm (at 0 N load) in the axial direction and apply a maximum force of 18 N at 0 μm displacement. With the

Fig. 2 MISSE 7 Space
tribometer schematic. **a** Single
space tribometer schematic with
all major components labeled.
The tribometer consists of a
monolithic biaxial force
transducer, loading flexure, and
a pin holding assembly that is
actuated by a piezoelectric
actuator. This applies a normal
force to the sample disk, which
is turned by a geared motor.
b Packaging for four space
tribometers onto a single base
plate as flown on MISSE 7b
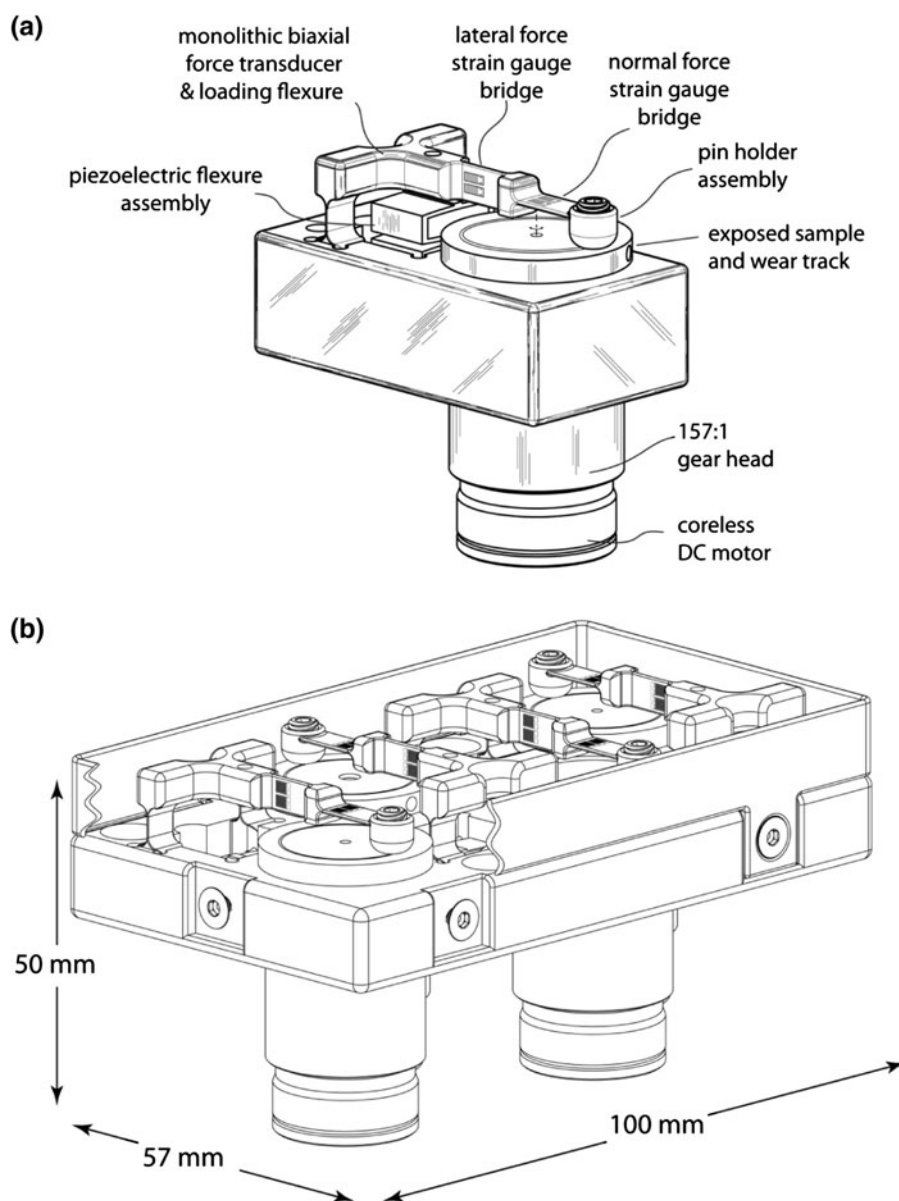
tribometer geometry, this yields a 1 N load and 500 µm displacement at the pin/disk interface. The piezo is $9.8 \times 12.8 \times 9$ mm in overall dimensions, has a mass of only 2 g, requires an excitation voltage between 0 and 150 V, has a stiffness of 0.23 N/µm, and a capacitance of 0.25 µF.

3.3.3 Motor/Spindle Assembly

A flat, coreless DC motor was selected from Maxon motors, due to the compact size, vacuum compatibility, and robustness. The motor was paired with a 157:1 gearbox that was lubricated with vacuum compatible grease. The high torque, slow speed, low power design afforded the opportunity to install eight tribometers on the MISSE 7 platform subject to power constraints.

3.3.4 Baseplate

All components of the tribometer are mounted to a common baseplate that is mounted directly onto the MISSE 7 platform. It was designed such that four tribometers fit onto a single 60×100 mm area. This base was made of 304 stainless steel, and securely fastened the flexures, motors, piezos, sidewall (a protective aluminum wall surrounding the tribometers as seen in Fig. 2b), and thermocouples. Open areas of the base between the tribometers housed several polymer samples to be exposed to the environment and analyzed and undergo tribological testing upon the return of the experiments. There are also several standoff washers between the base and the MISSE 7 platform that are coated with $MoS_2/Sb_2O_3/Graphite$; these washers serve

two purposes: to space the experiments off of the MISSE platform to insure adequate room for the motors and to be used as passive samples that can be tested upon return.

4 Experimental Protocol

Each orbit of the International Space Station lasts approximately 92 min. Periodically over the first half of 2010, the tribometers will run a set of 16 experiments of 1 min duration throughout an orbit. The schedule of experiments is based on the diurnal cycle of the International Space Station. Over the first week, the experiments are attempting to collect data during the following orbits: 1st, 2nd, 5th, 10th, 20th, 50th, and 100th orbits. After this first week on orbit, the experiments then begin to run once at 100 orbit intervals (about once a week) for the duration of the mission. As solid lubricants wear during operation, their lifetime is finite and running continuously may wear through the samples far too early in the mission. The spacing of every 100th orbit was selected as a compromise to study the effects of long-term exposure and provide significant amounts of on orbit data. Due to the limited power constraints the protocol is not to run the tribometers at the same time. Finally, on board memory is limited to 1 GB per tribometer, and we are saving a bolus of kHz data acquisition to the onboard memory along with processed and averaged data that is being telemetered back to ground through available NASA channels.

On a selected orbit, each tribometer on a given side (ram or wake) will run 16 one minute tests equally spaced throughout the orbit as shown in Fig. 3a. To insure that only one tribometer runs at a time, the tribometers (1, 2, 3, and 4) will run sequential 1 min cycles, followed by a 1 min break as shown in Fig. 3b. After this break, the testing repeats with tribometer 1 to complete the 16 one minute tests for each tribometer distributed over an entire orbit of the earth.

Each 1-min test starts with a period of unloading to zero the normal (F_N) and lateral (F_L) forces and account for any thermal drifts that may occur during the orbit. After zeroing, the experimental protocol is to perform seven complete revolution cycles in the clockwise direction (denoted by the subscript cw) followed by seven complete revolution cycles in the counterclockwise direction (denoted by the subscript ccw); finally the tribometers are unloaded and the force transducers collect data to measure any drift in the signal zeros. A typical voltage trace for a 1-min tribology experiment is shown in Fig. 3c. The sinusoidal behavior of the voltages is the result of the disk test surface not being normal to the axis of the motor causing variations in the height of the disk relative to the transducer which results in a fluctuation in normal force and consequent friction force.

The average friction coefficient, μ, for each 1-min experiment is a function of the average normal force ($\bar{F}_N$), the average friction lateral force for rotations in the clockwise ($\bar{F}_{L_{cw}}$) and counterclockwise ($\bar{F}_{L_{ccw}}$) directions; it is calculated according to Eq. 1.

$$\mu = \frac{\bar{F}_{L_{cw}} - \bar{F}_{L_{ccw}}}{2\bar{F}_N} \tag{1}$$

For the experimental design and instrumentation used on this tribometer embodiment, the uncertainty in forces was $u(F) = 15$ mN, and the normal load was nominally $F_N = 1$ N. From these conservative uncertainties, the uncertainty in friction coefficient is $u(\mu) = 0.01$ or less; Appendix 1 shows a detailed breakdown of the uncertainty. Subtracting the clockwise and counterclockwise lateral forces allows us to remove any bias errors from the system that arise from uncertain zeroing of the lateral force channel.

5 Material Selection

With such a rare opportunity for testing, material selection was a large responsibility that was not solely done by the authors; materials were determined by a number of collaborators within the research community and the aerospace industry (all gratefully acknowledged at the conclusion of the manuscript). This collaboration resulted in the selected flight materials as outlined in table 1. Four materials were selected for the ram face (R1–R4), and four materials were selected for the wake face (W1–W4); two materials are on both the ram and wake experiments.

Soft metals such as gold, silver, lead, and indium are materials that have been used as tribological materials in space for many years. Gold (R4) will be tested on the ram set of experiments; it is of particular interest as it is inert, oxidation resistant, and has been used as a solid lubricant in space. For this experiment we used a sapphire pin, which should also be stable in the LEO environment.

Polytetrafluoroethylene (PTFE) is a polymer that is well known for its stability and low friction characteristics. It is widely regarded as a candidate material for use in LEO; however, the high wear rates limit the number of applications. PTFE filled with alpha phase alumina nanoparticles has been shown to provide ultralow wear behavior (the wear rate has been shown to be reduced by almost 10,000 times [15, 16]). These PTFE nanocomposites at 10 wt% alumina loading will be examined on both the ram and wake environments (R1 and W1).

MoS_2 is a lamellar solid that has proven experience in a vacuum and space [17–25]. On the ram face a commonly used $MoS_2/Sb_2O_3/Au$ coating [21, 26] will be tested in part as a control sample given its proven experience but
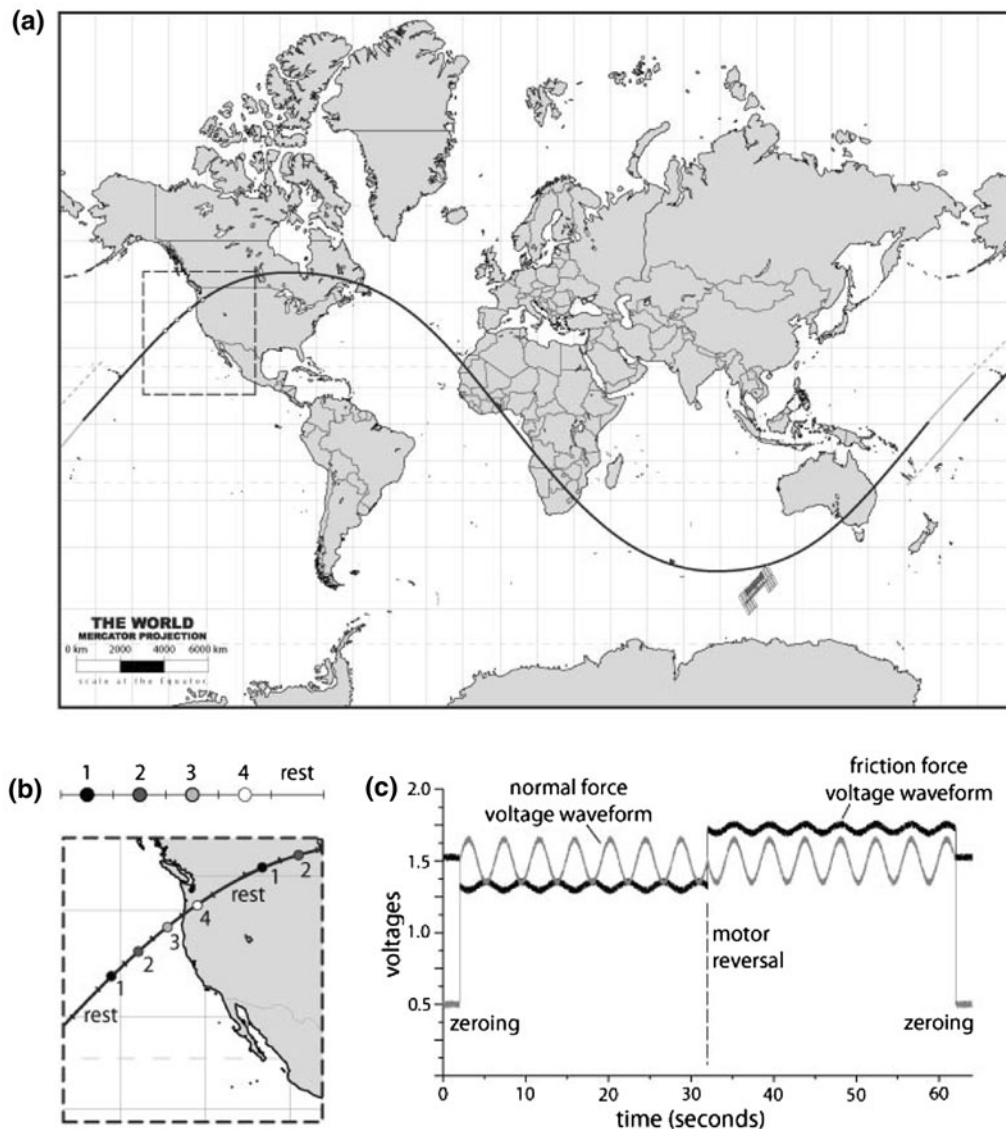
Fig. 3 Low earth orbit space tribometer on-orbit operations and experiment schedule. **a** The low earth orbit space tribometers are programmed to run one minute experiments at intervals throughout the space station's orbit. **b** The datum points (1, 2, 3, and 4) each represent a tribometer on the ram or wake side and shows the fraction of orbit that a single experiment would occupy. **c** The schedule is programmed to run one minute and a typical friction experimental voltage trace is shown. Each tribometer will run clockwise for 30 s and then counterclockwise for 30 with voltage zeroing at the beginning and end of each experiment

unmeasured performance in space. Recently multifunctional nanocomposites have been developed under a hypothesis of adaptive behavior to changing environments [27]. A $MoS_2/Sb_2O_3/C$ [24] composite coating will be tested on the wake face (W3). The role of carbon in similar films has been the subject of recent study [28, 29], and the susceptibility of attack from atomic oxygen is not a primary concern in higher orbits. The next generation "Chameleon" coatings are using continuous amorphous-nanocrystalline YSZ matrix surrounding nanoscopic inclusions of Au, MoS_2, and DLC. These coatings are showing promising results in the

laboratory and were selected for experiments on both the ram and wake faces (R2 and W2).

Hydrogenated diamond-like carbon (DLC) coatings are a class of materials that exhibit extremely low friction and wear with especially good performance in dry and vacuum conditions [30]. However, stability with respect to temperature and oxidation—key challenges for aerospace deployment—are critical limiting factors for conventional DLC's. Advanced DLC's formed by adding dopants represent a promising route to ameliorating these concerns. SiO-doped DLC enhances durability and thermal stability

Table 1 Results from ground testing in the NASA Marshall clean room after final assembly and integration of the tribometers on the MISSE 7b platform.

	Disk sample/coating	Ball material	Disk substrate	Preflight/cleanroom testing results			
				$\mu_{(avg)}$	$Fn_{(avg)}$ N	Cycles #	Distance (m)
RAM	$MoS_2/Au/Sb_2O_3$	440C	304 Stainless Steel	0.12	1	111	87.9
	$YSZ/Au/MoS_2/C$	440C	304 Stainless Steel	0.15	1.01	111	87.9
	$PTFE/nano-Al_2O_3$	440C	Bulk $PTFE/Al_2O_3$	0.16	1.06	73	57.8
	Gold	Ruby	Bulk gold	0.2	0.73	68	53.8
Wake	$MoS_2/Sb_2O_3/Graphite$	440C	304 Stainless Steel	0.12	0.98	72	57
	$PTFE/nano-Al_2O_3$	440C	Bulk $PTFE/Al_2O_3$	0.12	1.08	70	55.4
	$YSZ/Au/MoS_2/C$	440C	304 Stainless Steel	0.12	0.96	71	56.2
	DLC/SiO-doped	440C	304 Stainless Steel	0.18	0.8	67	53

The tribometers were run in lab environments of 22C at 24% relative humidity and followed the experimental protocol described in the text. The friction coefficients reported here are averages from the entire testing duration. All experiments had at least 1 h of sliding

as the Si atoms increase the tetrahedral bonding character within the film, and the high oxygen content stabilizes the film against further oxidative degradation. Macro- and nanoscale studies of SiO-doped DLC have demonstrated these desired property improvements [31–33] including through previous space exposure tests [34].

6 Closing Remarks

Eight pin-on-disk tribometers were developed and delivered to the International Space Station, they launched on November 16th 2009 aboard the STS-129 shuttle Atlantis. Four tribometers were installed facing forward (ram) and the other four tribometers were installed facing backwards (wake); forwards and backwards are relative to the space station velocity. These tribometers will run for approximately 8–14 months at which point they are scheduled to return (tentatively spring 2011). The tribometers activated on November 27th 2009 successfully began to run experiments and send data back from the International Space Station. The tribometers are also logging higher resolution data on orbit, and these data are being logged to an onboard non-volatile memory card that will return with the tribometers as part of the STS-134 mission. The experimental result and analysis of the samples from this mission will be presented in future publications after they return to earth.

Appendix 1: Uncertainty Analysis for the Space Tribometers

The uncertainty analysis for the friction coefficient follows the methods described by Burris and Sawyer [35] and Schmitz et al. [36]. To a reasonable approximation the uncertainty in the lateral directions is the same as the uncertainty in the normal direction, $u(F_L) = u(F_N) = u(F)$. In addition, the magnitude of the lateral forces during clockwise and counterclockwise rotations are approximately equal, $|F_{L_{cw}}| = |F_{L_{ccw}}| = |F_L|$. Hence,

$$u(\mu)^2 = \left(2\left(\frac{1}{2F_N}\right)^2 + \left(\frac{F_L}{F_N^2}\right)^2 \right) u(F)^2 \tag{2}$$

Upon simplification, and a substitution for the lateral force magnitude ($F_L = \mu F_N$), Eq. 2 can be simplified to give Eq. 3:

$$u(\mu)^2 = \frac{1 + 2\mu^2}{2F_N^2} u(F)^2 \tag{3}$$

Solving for uncertainty in the average friction coefficient is compactly given by Eq. 4. For low-friction materials, the uncertainty in friction coefficient is given by Eq. 5.

$$u(\mu) = \frac{u(F)}{F_N} \sqrt{\frac{1}{2} + \mu^2} \tag{4}$$

$$u(\mu) \approx \frac{u(F)}{\sqrt{2} F_N} \tag{5}$$

For the experimental design and instrumentation used on this tribometer embodiment, the uncertainty in forces was $u(F) = 15$ mN, and the normal load was nominally

$F_N = 1$ N. Thus, the uncertainty in friction coefficient is not better than $u(\mu) = 0.01$. This is a reasonable result and achievement considering design constraints placed on the hardware, but, as others have demonstrated in UHV, it is certainly possible to have lower uncertainties in friction coefficient [18, 37–40].

References

1. Yang, J.C., De Groh, K.K.: Materials issues in the space environment. Mrs Bull. **35**, 12–16 (2010)
2. Edwards, D.L., Tighe, A.P., Eesbeek, M.V., Kimoto, Y., De Groh, K.K.: Overview of the natural space environment and ESA, JAXA, and NASA materials flight experiments. Mrs Bull. **35**, 25–34 (2010)
3. De Groh, K.K., Banks, B.A., McCarthy, C.E., Rucker, R.N., Roberts, L.M., Berger, L.A.: MISSE 2 peace polymers atomic oxygen erosion experiment on the international space station. High Perform Polym. **20**, 388–409 (2008)
4. Dever, J.A., Miller, S.K., Sechkar, E.A., Wittberg, T.N.: Space environment exposure of polymer films on the materials international space station experiment: Results from MISSE 1 and MISSE 2. High Perform Polym. **20**, 371–387 (2008)
5. Walters, R.J., Garner, J.C., Lam, S.N., Vasquez, J.A., Braun, W.R., Ruth, R.E., Messenger, S.R., Lorentzen, J.R., Bruninga, R., Jenkins, P.P., Flatico, J.M., Wilt, D.M., Piszczor, M.F., Greer, L.C., Krasowski, M.J.: Materials on the international space station - forward technology solar cell experiment. Mat. Sci. Eng. B-Solid. **116**, 257–263 (2005)
6. Jenkins, P.P., Walters, J.R., Michael, J.K., John, J.C., Perry, G.B., John, A.V., Denis, R.M., Susie, N.L., William, R.B., Robert, S., Norman, F.P., Joseph, M.F., Lawrence, C.G., Karen, B.G., William, H.K., and Pippin, H.G.: MISSE 7: building a permanent environmental testbed for the international space station. AIP,(2009)
7. Sawyer, W.G., Wahl, K.J.: Accessing inaccessible interfaces: In situ approaches to materials tribology. Mrs Bull. **33**, 1145–1148 (2008)
8. Wahl, K.J., Sawyer, W.G.: Observing interfacial sliding processes in solid-solid contacts. Mrs Bull. **33**, 1159–1167 (2008)
9. Banks, B.A., Miller, S.K., de Groh, K.K.: Low earth orbital atomic oxygen interactions with materials. In: Second International Energy Conversion Engineering Conference. Providence, Rhode Island (2004)
10. Grossman, E., Gouzman, I.: Space environment effects on polymers in low earth orbit. Nucl. Instrum. Meth. B. **208**, 48–57 (2003)
11. ASTM: Standard solar constant and zero air mass solar spectral irradiance tables. ASTM E490 (2006)
12. ASTM: Standard tables for reference solar spectral irradiances: Direct normal and hemispherical on 37° tilted surface. ASTM G173 - 03e1)
13. Dever, J.A.: Low earth orbital atomic oxygen and ultraviolet radiation effects on polymers. E-5943; NAS 1.15:103711; NASA-TM-103711 (1991)
14. Miles, J.W.: On structural fatigue under random loading. J. Aeronaut. Sci. **21**, 753–762 (1954)
15. Burris, D.L., Sawyer, W.G.: Improved wear resistance in alumina-PTFE nanocomposites with irregular shaped nanoparticles. Wear **260**, 915–918 (2006)
16. Mcelwain, S.E., Blanchet, T.A., Schadler, L.S., Sawyer, W.G.: Effect of particle size on the wear resistance of alumina-filled PTFE micro- and nanocomposites. Tribol. T. **51**, 247–253 (2008)

17. Aouadi, S.M., Paudel, Y., Luster, B., Stadler, S., Kohli, P., Muratore, C., Hager, C., Voevodin, A.A.: Adaptive Mo2N/MoS2/Ag tribological nanocomposite coatings for aerospace applications. Tribol. Lett. **29**, 95–103 (2008)
18. Martin, J.M., Le.Mogne, T., Boehm, M., Grossiord, C.: Tribochemistry in the analytical UHV tribometer. Tribol. Int. **32**, 617–626 (1999)
19. Muratore, C., Voevodin, A.A.: Molybdenum disulfide as a lubricant and catalyst in adaptive nanocomposite coatings. Surf. Coat. Tech. **201**, 4125–4130 (2006)
20. Roberts, E.W.: Ultralow friction films of MoS2 for space applications. Thin Solid Films **181**, 461–473 (1989)
21. Scharf, T.W., Kotula, P.G., Prasad, S.V.: Friction and wear mechanisms in MoS2/Sb2O3/Au nanocomposite coatings. Acta Mater. **58**, 4100–4109 (2010)
22. Tagawa, M., Muromoto, M., Hachiue, S., Yokota, K., Ohmae, N., Matsumoto, K., Suzuki, M.: Hyperthermal atomic oxygen interaction with MoS2 lubricants and relevance to space environmental effects in low earth orbit - effects on friction coefficient and wear-life. Tribol. Lett. **18**, 437–443 (2005)
23. Voevodin, A.A., Zabinski, J.S.: Nanocomposite and nanostructured tribological materials for space applications. Compos. Sci. Technol. **65**, 741–748 (2005)
24. Zabinski, J.S., Bultman, J.E., Sanders, J.H., Hu, J.J.: Multi-environmental lubrication performance and lubrication mechanism of MoS2/Sb2O3/C composite films. Tribol. Lett. **23**, 155–163 (2006)
25. Fleischauer, P.D., Hilton, M.R., Raju, B.K., Vedachalam, N., Wei, L.Y., Huang, K.W., Nishimura, M.: International applications of space tribology. Tribol. Int. **23**, 135–147 (1990)
26. Hamilton, M.A., Alvarez, L.A., Mauntler, N.A., Argibay, N., Colbert, R., Burris, D.L., Muratore, C., Voevodin, A.A., Perry, S.S., Sawyer, W.G.: A possible link between macroscopic wear and temperature dependent friction behaviors of MoS2 coatings. Tribol. Lett. **32**, 91–98 (2008)
27. Voevodin, A.A., Fitz, T.A., Hu, J.J., Zabinski, J.S.: Nanocomposite tribological coatings with "Chameleon" Surface adaptation. J. Vac. Sci. Technol. A. **20**, 1434–1444 (2002)
28. Baker, C.C., Chromik, R.R., Wahl, K.J., Hu, J.J., Voevodin, A.A.: Preparation of chameleon coatings for space and ambient environments. Thin Solid Films **515**, 6737–6743 (2007)
29. Chromik, R.R., Baker, C.C., Voevodin, A.A., Wahl, K.J.: In situ tribometry of solid lubricant nanocomposite coatings. Wear **262**, 1239–1252 (2007)
30. Erdemir, A., Donnet, C.: Tribology of diamond-like carbon films: Recent progress and future prospects. J. Phys. D Appl. Phys. **39**, R311–327 (2006)
31. Bhaskaran, H., Gotsmann, B., Sebastian, A., Drechsler, U., Lantz, M.A., Despont, M., Jaroenapibal, P., Carpick, R.W., Chen, Y., Sridharan, K.: Ultralow nanoscale wear through atom-by-atom attrition in silicon-containing diamond-like carbon. Nat. Nanotechnol. **5**, 181–185 (2010)
32. Bares, J.A., Sumant, A.V., Grierson, D.S., Carpick, R.W., Sridharan, K.: Small amplitude reciprocating wear performance of diamond-like carbon films: Dependence of film composition and counterface material. Tribol. Lett. **27**, 79–88 (2007)
33. [33].Scharf, T.W., Ohlhausen, J.A., Tallant, D.R., and Prasad, S.V.: Mechanisms of friction in diamondlike nanocomposite coatings. J. Appl. Phys. 101 (2007)
34. Prasad, S.V.: Personal communication. (2009)
35. Burris, D.L., Sawyer, W.G.: Addressing practical challenges of low friction coefficient measurements. Tribol. Lett. **35**, 17–23 (2009)
36. Schmitz, T.L., Action, J.E., Ziegert, J.C., Sawyer, W.G.: The difficulty of measuring low friction: Uncertainty analysis for friction coefficient measurements. J. Tribol.-T Asme. **127**, 673–678 (2005)

37. Gao, F., Erdemir, A., Tysoe, W.T.: The tribological properties of low-friction hydrogenated diamond-like carbon measured in ultrahigh vacuum. Tribol. Lett. **20**, 221–227 (2005)

38. Kim, H.I., Lince, J.R., Eryilmaz, O.L., Erdemir, A.: Environmental effects on the friction of hydrogenated dlc films. Tribol. Lett. **21**, 53–58 (2006)

39. Martin, J.M., LeMogne, T.: Tribo-oxidation in UHV experiments. Analusis. **25**, M28–30 (1997)

40. Singer, I.L., LeMogne, T., Donnet, C., Martin, J.M.: Friction behavior and wear analysis of sic sliding against Mo in SO_2, O_2 and H_2S at gas pressures between 4 and 40 pa. Tribol. T. **39**, 950–956 (1996)